FREQUENCY MAP MEASUREMENTS AT THE TPS

C. H. Chen[†], M. S. Chiu, J. Y. Chen, F. H. Tseng, B. Y. Chen, B. Y. Huang, T. W. Hsu, W. Y. Lin,
C. C. Kuo, H. J. Tsai, Y. C. Liu, P. J. Chou
National Synchrotron Radiation Research Center, Hsinchu, Taiwan

Abstract

The Taiwan Photon Source (TPS) has been operated now for several years since its successful commissioning in December 2014 and has achieved reliable routine operation up to 500 mA with more than 10 hrs beam lifetime. Dynamic aperture (DA) measurements and associated frequency map analyses (FMA) at the TPS reveal beam dynamics behavior with and without insertion devices. A preliminary study based on turn-by-turn beam position monitor (BPMs) is presented in this paper.

INTRODUCTION

The TPS is a 3 GeV 3rd-generation synchrotron light source in Hsinchu, Taiwan. The lattice structure consists of 24 DBA cells with 6-fold symmetry and its natural emittance is 1.6 nm-rad. The TPS was successfully commissioned in the end of 2014 [1]. The TPS has been operated for users since completion of the commissioning with seven insertion devices (IDs) [2], superconducting cavities and now a beam current up to 500 mA. Its linear optics was implemented and corrected with LOCO [3]. The peak-to-peak beta-beating and linear coupling had been corrected to below 1 % and 0.1 % for routine user operation, respectively [4]. To further understand the nonlinear beam dynamics behavior, we conducted beam measurements and analyzed the frequency maps such that the operation conditions could be optimized.

EXPERIMENTAL SETTING

A lattice with working point (υ_x=26.14, υ_y=14.24) and chromaticity (ξ_x=0.7, ξ_y=0.8), while ID is open, is utilized in this study. The multi-bunch mode injection is adjusted for 10 buckets, 20 nsec bunch trains and a 0.3 mA bunch current.

Both, horizontal and vertical scrapers and pinger magnets are installed in the storage ring near the injection section of the TPS. As shown in Fig. 1, scrapers, located 1.38 m downstream of the injection kicker magnet (K3), can function to determine the transverse aperture. Both pinger magnets are placed 1.37 m downstream of the scraper. Two pinger magnets, with a pulse duration shorter than twice of the storage ring revolution time, are used to excite the beam. Because the revolution time for the TPS is 1.7 µsec, a full half-sine pulse duration in the TPS pinger of 3-µsec guarantees a one-turn beam excitation.

This study aims on nonlinear phenomena associated with IDs when their gaps are open or closed. There are seven IDs in service for users operation and their usual operational status are determined by experimental

conditions as listed in Fig. 1, while three more in-vacuum undulators are installed but not available for users yet.

port	ID	gap open / closed (mm)
5	IU22	40/7
9	IU22A	40/7
9	IU22B	40/40
21	IUT22	40/7
23	IU22	40/7
25	IU22A	40/7
25	IU22B	40/40
41	EPU48A	65/65
41	EPU48B	65/28
45	EPU46	65/28
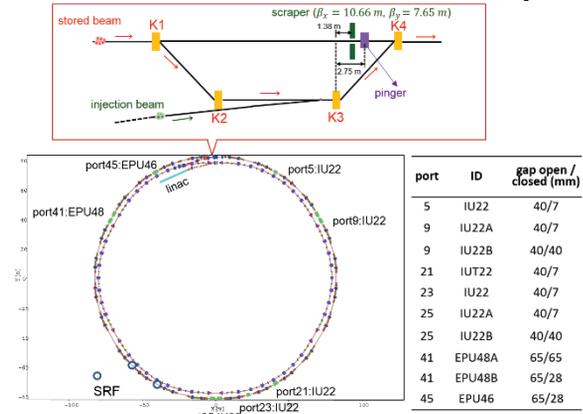
Figure 1: Layout of the TPS: the scrapers and pinger magnets are shown in the upper enlarged picture. The status of IDs, being open or closed, are listed in the inserted table.

The BPM signals from Libera electronics [5] could acquire the beam transverse positions turn-by-turn with a 3 µm rms resolution. However, the non-linear BPM responses are explored near an amplitude of ± 4 mm and are saturated at ± 6 mm. In order to find the linearity between amplitudes and BPM responses, the stored beam was perturbed by varying the pinger strength until the beam got lost. The amplitudes are normalized with the optical parameters at the scraper indicating an exact amplitude at a horizontal beta-function of β_x=10.66 m and a vertical beta-function of β_y= 7.65 m. Some normalized amplitudes (black circle) within 4 mm are picked for linear fitting to find the linear relation (black curve) between amplitude and pinger strength as shown by the formulas in Fig. 2.
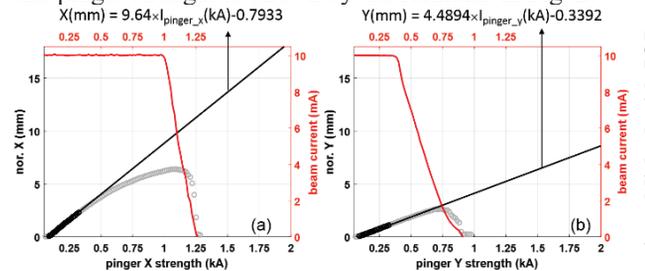
Figure 2: Linear amplitude fit for both pinger magnets. The amplitudes are normalized to scraper positions (circles) versus horizontal (a) and vertical (b) pinger strength. Black circles indicate the linear range for fitting.

The measured integral magnetic fields of the pinger magnets in the lab are linear to the excitation currents. The extreme normalized amplitudes at the beam current loss point (red) indicate an aperture limitation of 11.5 mm and

---
† chen.chiahsiang@nsrrc.org.tw

3.5 mm in the horizontal and vertical plane at scraper position, respectively.

MEASUREMENTS

Transverse Aperture

Moving scraper blades into the beam partially scrapes beam leading to a reduced beam lifetime. In Fig. 3, the product of bunch current and lifetime in the single bunch mode as a function of scraper position is shown, which reaches turning point when the scraper blades are close to beam dynamic aperture or physical aperture, which occurs at apertures of about 12 mm (horizontal) and 3 mm (vertical). The horizontal physical aperture acceptance at scraper position is about 21 mm (limited by septum edge), and vertical physical aperture is about 5.4 mm when IU gaps are closed to 7 mm, or 6.0 mm when IU gaps are open (limited by EPU chambers).
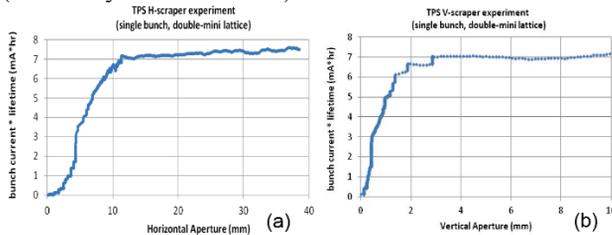
Figure 3: Using scrapers to determine the horizontal (a) and vertical (b) aperture.

Tune Shift with Amplitude

When the ID gaps are open, Fig. 4 demonstrates the betatron tune excitations by both pinger magnets. The precise betatron tunes are calculated with the help of NAFF [6] with the first 512 turn-by-turn BPM data and the results are similar to simulations [7]. The horizontal tune in Fig. 4(a) drops to 26.125 near a horizontal amplitude of 8 mm due to being close to the 8th resonance as shown in Fig.8(a), but a vertical excitation does not cause the tune to change significantly in Fig. 4 (c) and (d).
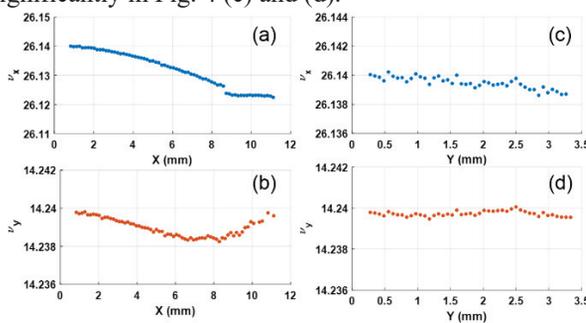
Figure 4: (a,b) show measured tune shifts as a function of horizontal amplitude ; (c,d) are tune shifts vs. vertical amplitude.

Tune Shift with Energy

Due to small first-order and large second-order momentum compaction factors, the relation between relative momentum deviation and RF frequency is expressed by Eq. (1). By changing the RF frequency setting to have the momentum deviation in between $\pm$ 6% in this measurement, we find beam loss near nodes of multi-resonance lines about -5 % and 5 % as seen by black circles in Fig. 5(b).

$$\delta = \frac{\Delta E}{E} = -\frac{\alpha_1}{2\alpha_2}\left(1 - \sqrt{1 - \frac{4\alpha_2}{\alpha_1}\frac{\Delta f_{rf}}{f_{rf}}}\right) \quad (1)$$

In Eq. (1), α_1 =2.4E-4 and α_2 =2.5E-3 are the 1st and 2nd order momentum compaction factor, Δf_{rf} the shift of the RF-frequency f_{rf}.
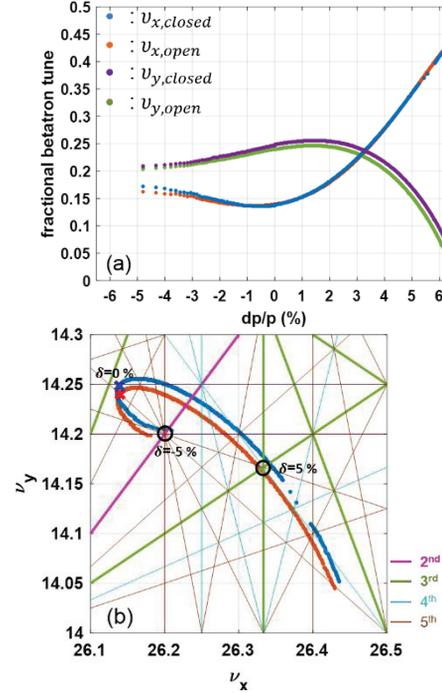
Figure 5: (a) Measured tune shifts versus energy deviation and (b) measured frequency map for off-momentum beams when the ID gaps are open (red dot) and closed (blue dot).

Beam Loss Rate

Many analyses for the beam loss rate, frequency map and dynamic aperture depend on a large volume of turn-by-turn BPM observations. These high density maps are formed from 81 horizontal and 61 vertical equal-distance meshes for the case of open ID gaps, and 71 horizontal and 55 vertical meshes for closed ID gaps, respectively. The beam loss rate map does not only display the distribution for the surviving beam but also indicates the transverse aperture clearly. When the ID gap is open, a horizontal aperture of 11.5 mm and a vertical aperture of 3.5 mm is obtained with the pinger magnets, which agrees with scraper results. Apertures of 10 and 3.4 mm in the horizontal and vertical plane are observed when the ID gaps are closed.

The beam loss rate $R_{m,n}$ is defined in Eq. (2) and is shown by the color used in Fig. 6, where m and n is the m_{th} and n_{th} step of the pinger strength in the horizontal and vertical plane. $I_{m,n}$ is the beam current at that time.

$$R_{m,n} = \frac{I_{(m,n)} - I_{(m+1,n+1)}}{I_{(m,n)}}, \quad (2)$$
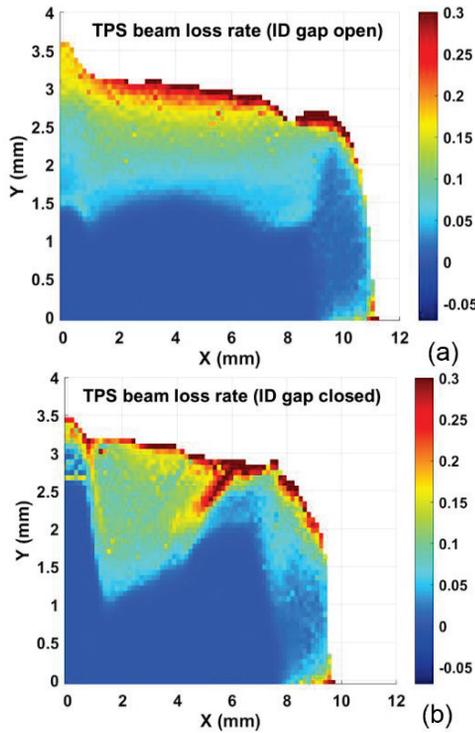
Figure 6: Beam loss rate maps for ID gaps being open (a) or closed (b)

Dynamic Aperture and Frequency Map

The tune diffusion (D) is shown by colored dots defined by $D = log_{10}\sqrt{(\Delta v_x^2 + \Delta v_y^2)}$, where $\Delta v = v_{1\text{-}512th} - v_{513\text{-}1024th}$ is the tune spread for the first 512 turns and the next 512 turns in the NAFF process.
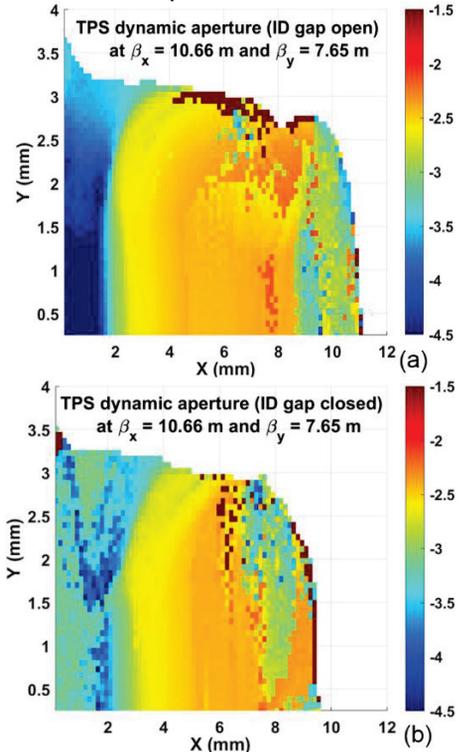
Figure 7: Measured dynamic apertures while ID gaps are open (a) or closed (b).

The working tunes, marked with red crosses, are v_x=26.1399 and v_y= 14.2398 for open ID gaps in Fig8(a), v_x=26.1394 and v_y=14.2490 for closed gaps in Fig8(b). For larger horizontal and vertical amplitudes, see Fig. 7(a) and 8(a), the tunes diffuse strongly to v_x=26.123 and v_y=14.245, or toward a coupled third order resonance line as the horizontal amplitude approaches 8 mm. In Fig. 8(b), the tune distributions are close to main resonances, especially close to the most unstable tunes near the nodes of multi-resonance lines. Based on this map, we know well how to keep away from those resonant hot zones by adjusting the working tune when the gaps are closed.
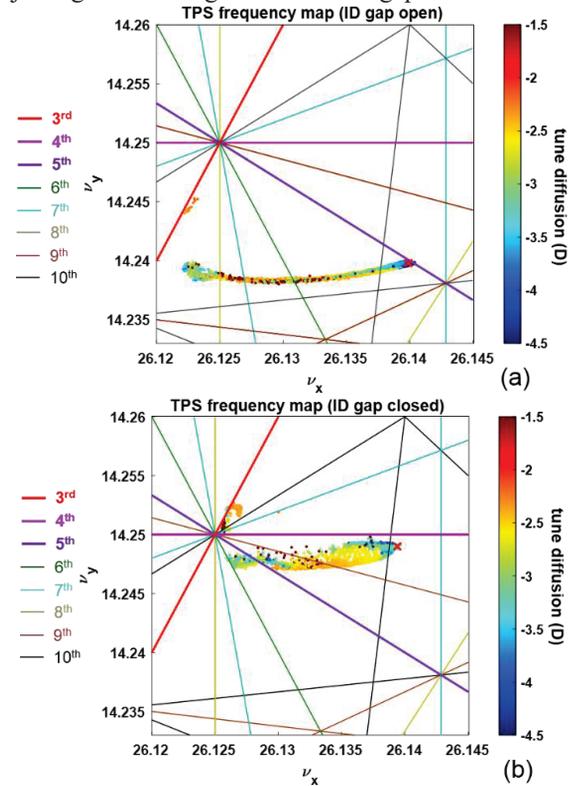
Figure 8: Measured frequency maps with resonances while ID gaps are open (a) or closed (b). Lower order resonances (3rd, 4th and 5th) are shown in bold lines.

CONCLUSION

Transverse dynamic apertures of 11.5 mm (x), 3.5 mm (y) mm and 10 mm (x), 3.4 mm (y) mm are observed for ID gaps being open or closed, respectively at scraper position (β_x =10.66 m, β_y =7.65 m). The precise determination of the dynamic apertures and the high resolution of frequency maps presented here for the first time. This precise systematic diagnostic for FMA and DA could be used for optimizing routine operation in the TPS.

ACKNOWLEDGMENTS

REFERENCES

[1] C.-C. Kuo *et al.*, "Commissioning of the Taiwan Photon Source", in *Proc. IPAC'15*, Richmond, VA, USA, May 2015, pp. 1314-1318. `doi:10.18429/JACoW-IPAC2015-TUXC3`

[2] M.-S. Chiu *et al.*, "The Commmissioning of Phase-I Insertion Devices in TPS", in *Proc. IPAC'16*, Busan, Korea, May 2016, pp. 3360-3362. `doi:10.18429/JACoW-IPAC2016-THPMB050`

[3] J. Safranek, "Experimental determination of storage ring optics using orbit response measurements", *Nuclear Instruments and Methods in Physics Research A*, 388, 27–36, 1997.

[4] F. H. Tseng *et al.*, "Optics Calibration During Commissioning of the Taiwan Photon Source", in *Proc. IPAC'16*, Busan, Korea, May 2016, pp. 3357-3359. `doi:10.18429/JACoW-IPAC2016-THPMB049`

[5] Libera Brilliance+, Electron Beam Position Processor: User manual, 2013, Solkan. Available at `http://www.i-tech.si/support/technical-documentation`.

[6] J. Laskar. "The measure of chaos by the numerical analysis of the fundamental frequencies. Application to the standard mapping", *Physica D: Nonlinear Phenomena*, 388, 253-269, 1992.

[7] M. S. Chiu *et al.*, "Optimization and measurement on the double mini-betay lattice in the tps storage ring", presented at the IPAC'19, Melbourne, Australia, May 2019, paper TUPGW071, this conference.